

# Chiral-to-Chiral Communication in Polymers: A Unique Approach to Control both Helical Sense and Chirality at the Periphery

Katherine Cobos, Emilio Quiñoá, Ricardo Riguera, Félix Freire

## Accepted Manuscript

This is the Accepted Manuscript version of a Published Work that appeared in final form in Journal of the American Chemical Society, Copyright © 2018 American Chemical Society after peer review and technical editing by the publisher. To access the final edited and published work see: <https://pubs.acs.org/doi/10.1021/jacs.8b07782>

## How to cite:

Cobos, K., Quiñoá, E., Riguera, R., & Freire, F. (2018). Chiral-to-Chiral Communication in Polymers: A Unique Approach To Control Both Helical Sense and Chirality at the Periphery. Journal Of The American Chemical Society, 140(38), 12239-12246. doi: 10.1021/jacs.8b07782

## Copyright information:

© 2018 American Chemical Society

# Chiral-to-Chiral Communication in Polymers: A Unique Approach to Control both Helical Sense and Chirality at the Periphery

Katherine Cobos, Emilio Quiñoá, Ricardo Riguera,\* Félix Freire\*

Centro Singular de investigación en Química Biolóxica e Materiais Moleculares (CiQUS) and Departamento de Química Orgánica, Universidade de Santiago de Compostela, E-15782 Santiago de Compostela, Spain

Supporting Information Placeholder

**ABSTRACT:** A novel approach to the classical Sergeants and Soldiers effect, using chiral Sergeants and chiral Soldiers, allow controlling both helical and external chirality in helical polymers. In the systems here reported it is possible to induce the same helical sense (*M* or *P*) from any of the two enantiomers of a chiral pendant group ["chiral Soldier", major component; i.e., (*R*)- or (*S*)-**1**] when they face a single enantiomer of an appropriate "chiral Sergeant" [minor component; i.e., (*S*)-**2**]. For instance, copolymer series poly-[(*R*)-**1**<sub>*r*</sub>-co-(*S*)-**2**<sub>(*l,r*)</sub>], poly-[(*S*)-**1**<sub>*r*</sub>-co-(*S*)-**2**<sub>(*l,r*)</sub>] and poly-[(*rac*)-**1**<sub>*r*</sub>-co-(*S*)-**2**<sub>(*l,r*)</sub>] adopt the same *P* helix despite the major component shows opposite absolute configurations. This chiral to chiral communication effect is transmitted by the stabilization of different conformations in each enantiomeric form of the Soldier. As a result, this groundbreaking approximation to the Sergeants and Soldiers effect allows preparing a single-handed helix—which only depends on the Sergeant's configuration—with different chiralities on the helix periphery. Thus, a *P* helix can be decorated with the (*R*)-, (*S*)- or even a racemic mixture of the chiral Soldier. Changes on the absolute configuration of the Sergeant will permit to obtain the opposite *M* helix, which can also be decorated with the (*R*)-, (*S*)- or the racemic mixture of the chiral Soldier.

## INTRODUCTION

The secondary structure of a helical polymer is related to the interactions between the monomers that constitute the polymeric chain.<sup>1</sup> In the case of copolymers formed by the combination of chiral and achiral monomers, this interaction may occur through a conformational communication mechanism resulting in a chiral amplification phenomenon. In such a case, it is found that the presence of a small amount of the chiral monomer (minor component) is capable of dominating the secondary structure of the whole copolymer chain by inducing a certain orientation in the achiral units (major

component). This chiral amplification phenomena is denoted as the "Sergeants and Soldiers effect"<sup>2</sup> and in practical terms, it means that the introduction of a small amount of a chiral unit ("Sergeant") within a polymer formed by achiral monomers ("Soldiers") will produce the formation of either *P* or *M* helices in the resulting copolymer chain depending on the chirality of the Sergeant used. This approach is very convenient to obtain functional helical polymers folded into a single handed *P* or *M* helix, because doping an inexpensive achiral chain with a small amount of an expensive chiral monomer provides the functional helicity—helices acting as chiral stationary phases,<sup>3</sup> chiral catalysts,<sup>4</sup> chiral nanocontainers<sup>5</sup>— that otherwise would be produced from a more expensive fully chiral homopolymer.

In our group, we became interested on the possibility to extend and also improve the helical function of a poly(phenylacetylene) (PPA) not only by controlling the helicity of the polymer (*P*/*M*) but also by taming simultaneously the chiral pendants used as Soldiers.<sup>2a</sup> Thus, while the helical sense of the polymer will be commanded by the chirality of the Sergeant, the chirality on the periphery of the helix will depend on the intrinsic chirality of the Soldier.

In this way, four different diastereoisomeric copolymers could be prepared from a chiral Sergeant (Sgt.) and a chiral Soldier (Sold.) —[poly-[(*R*/*S*)-Sergeant-co-(*R*/*S*)-Soldier]—. In these copolymers, the helical sense will be defined by the chirality of the Sergeant, while the chirality on the surface of the helix will depend on the chirality of the Soldier. For instance, if the (*R*)-Sgt. commands a left handed (*M*)-helix, both the (*R*)- and (*S*)- enantiomers of the Soldier will adopt the same *M* helix although their intrinsic chiralities are the opposite (Figure 1a). Similar situation should be founded if the enantiomeric form of the Sergeant [i.e. (*S*)-Sgt.] is used to induce a single-handed helix, although in this case a *P* helix should be generated (Figure 1b).

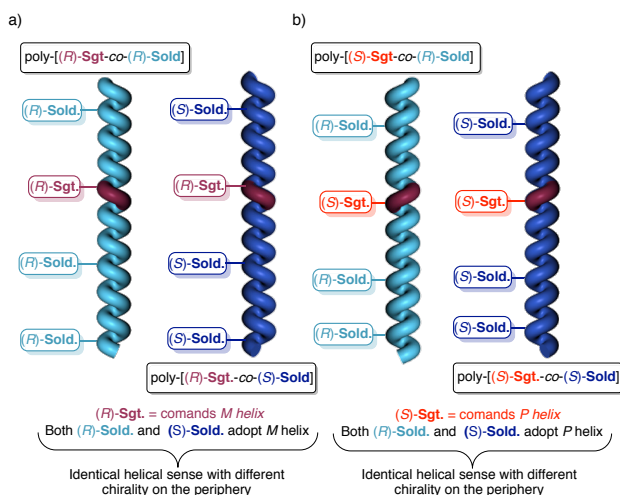


**Figure 1.** Conceptual representation of the chiral to chiral Sergeants and Soldiers effect using a Sergeant with either the (a) (R)- or (b) (S)-configuration. [Sgt = Sergeant, Sold = Soldier]

Thus, our approach focuses on the preparation of PPAs formed by two chiral components that establish communication between them. One is designed to control the helical sense (*P/M*) while the other is selected to tune the [(*R*-)/(*S*-)] configuration at the periphery of the helix.

In a first attempt, we explored the chiral-to-chiral communication mechanism in some PPAs copolymers.<sup>2a</sup> Those initial studies allowed us to elucidate the communication pathway between the two monomers, and the role played by their absolute configuration in the process of helical sense enhancement. As a result, we found that in order to have an effective (chiral) Sergeant to (chiral) Soldier effect, the two monomeric units must comprise the following requirements: a) the corresponding homopolymers must present similar helical scaffolds (i.e., *cis-cisoidal* or *cis-transoidal*), b) the Soldier must be conformationally flexible (i.e., homopolymer with weak polyenic band in CD), and c) the Sergeant must have a clearly predominant conformation (i.e., homopolymer with strong polyenic CD signature).<sup>2a</sup>

Nevertheless, although PPA copolymers prepared in accordance with those conditions showed high chiral amplification via the Sergeant and Soldier effect, the amplification phenomena observed follows an “abnormal” effect.<sup>2a, 2d, 6</sup> In the copolymer series studied, we observed that the Soldier—not the Sergeant!—was the component commanding the helical sense of the copolymer. Thus, the Sergeant, acting as a “chiral dopant”, is used to trigger the Soldier, which is activated in the same way (identical conformation activated in all cases) independently on the absolute configuration of the Sergeant—[(*R*-), (*S*-)]—, but producing opposite helical senses following the Soldier’s absolute configuration.<sup>2a</sup> Therefore, in those copolymer series, the chirality of the Soldier is the one that commands the helical sense of the copolymer. For instance, *M* helices are commanded by the (*R*)-Sold. — $M_{\text{helix1}}$  [(*R*)-Sgt<sub>minor</sub>/*(R)*-Sold<sub>major</sub>];  $M_{\text{helix2}}$  [(*S*-

Sgt<sub>minor</sub>/*(R)*-Sold<sub>major</sub>]— and *P* helices are commanded by the enantiomeric form [(*S*-)] of the Soldier — $P_{\text{helix1}}$  [(*R*)-Sgt<sub>minor</sub>/*(S)*-Sold<sub>major</sub>;  $P_{\text{helix2}}$  [(*S*)-Sgt<sub>minor</sub>/*(S)*-Sold<sub>major</sub>]—. As a result, two helices are obtained according to the absolute configuration of the major component: the Soldier (“chiral coalition effect”, Figure 2).

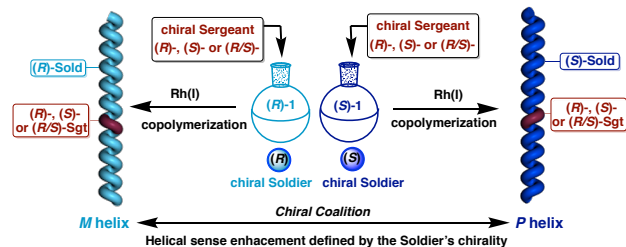


**Figure 2.** Schematic representation of the chiral coalition effect.

Herein, we will show a chiral PPA copolymer that follows the “classical” Sergeant and Soldier effect and fulfill our expectations: its *P/M* helical sense is exclusively determined by the chirality of the Sergeant, independently of the chirality of the Soldier, which will determine the chirality of the helix periphery—(*R*-), (*S*-), while the chirality at periphery of the helix is determined by the (*R*-) or (*S*-) absolute configuration of the Soldier. Moreover, modulation of the conformation of the Soldier by the presence of external stimuli—e.g., metal ions— will allow us to perform helix inversion between helical enhanced copolymers without changing the absolute configuration of the Sergeant.

## RESULTS AND DISCUSSION

To perform these studies we selected as chiral Soldiers the 4-ethynylanilides of (*R*-) or (*S*-) $\alpha$ -methoxy- $\alpha$ -phenylacetic acid (MPA) [monomers (*R*-) or (*S*-)**1**] (Figure 3),<sup>2a, 7</sup> and as chiral Sergeant the 4-ethynylanilide of the (*S*-) $\alpha$ -9-anthryl- $\alpha$ -methoxyacetic acid (9-AMA) [monomer (*S*-)**2**], that differs from monomer **1** in the replacement of the phenyl ring by an anthryl group (Figure 3a).

Monomer **1** [(*R*-) or (*S*-)] is known to be constituted by an equilibrium of two conformations at the O=C-C-O bond—*ap/sp*— in a 1:1 ratio (Figure 3b).<sup>7e</sup> In the corresponding polymers [i.e., poly(*R*-)**1** and poly(*S*-)**1**], the pendants adopt the same conformational equilibrium and therefore, equal amounts of the induced right- and left-handed helices. As a result, poly(*R*-)**1** and poly(*S*-)**1** adopt a *cis-cisoidal* helix, which are optically inactive (null CD) and, in spite of their stereogenic carbon centre. Therefore, these polymers behave as helical racemic from a macroscopic point of view<sup>7e</sup> (Figure 3c).

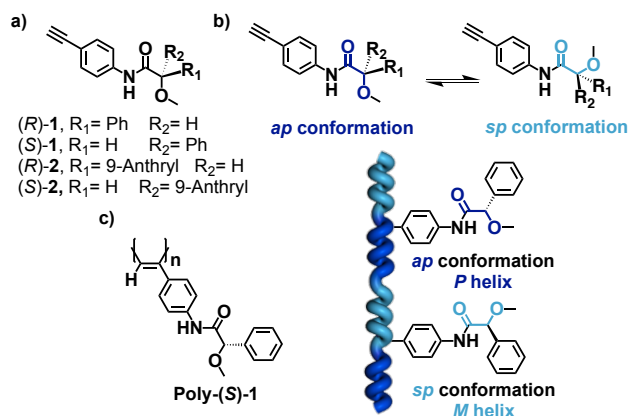


**Figure 3.** a) Structure of monomers (R)-1, (S)-1, (R)-2 and (S)-2. b) Conformational equilibrium between *ap* and *sp* conformations. c) Structure of poly-(S)-1 showing the presence of two different conformers at the MPA moieties responsible for the coexistence of the two helical senses in the polymer.

On the other hand, the amides of 9-AMA (monomers 2) are known to adopt a preferred *ap* conformation at the O=C-C-O bond (Figure 4a), both in solution and in solid state as confirmed by CD, NMR and X-ray<sup>8</sup> (Figure 4a and SI).

### Synthesis, structure and properties of poly-2

Polymerization of monomer (S)-2 with a Rh(I) catalyst, [Rh(nbd)Cl]<sub>2</sub> (nbd=2,5-norbornadiene), afforded poly-(S)-2 in good yield (> 90%) and with a high *cis* content of double bonds as determined by <sup>1</sup>H NMR and Raman (vinyl protons at δ = 5.8–6.2 ppm in NMR; Raman bands at 1576, 1345, 1023 cm<sup>-1</sup>).<sup>9, 10</sup> CD spectra of poly-(S)-2 measured in different solvents (polar/non polar) indicated that poly-(S)-2 adopts a preferred helical sense which is directly related to the presence of the major *ap* conformation at the pendant group (Figures 4b, c).

The presence of the major *ap* conformer in poly-(R)-2 and poly-(S)-2, was confirmed by the helical inversion observed after addition of Ba(ClO<sub>4</sub>)<sub>2</sub> to a chloroform solution of the polymer (chelation with M<sup>2+</sup> favors the *sp* conformation, Figure 4d), and by the helical enhancement observed after addition of salts of monovalent metal ions such as LiClO<sub>4</sub> that favor the *ap* conformation<sup>8</sup> (see SI for details).

Next, structural studies —CD, Raman, DSC and AFM— were performed to obtain the secondary structure of these polymers (Figure 5).<sup>11</sup> High resolution AFM images of a well-ordered monolayer of poly-(S)-2 revealed the presence of well-packed polymer chains aligned parallel to each other. From these images, the helical pitch (2.5 nm), packing angle (65°) and the sense of the external part of the helix (*P*<sub>ext</sub>) were determined (Figure 5a). These data are in full agreement with a *cis-cisoidal* backbone that was further confirmed by DSC studies (Figure 5b).

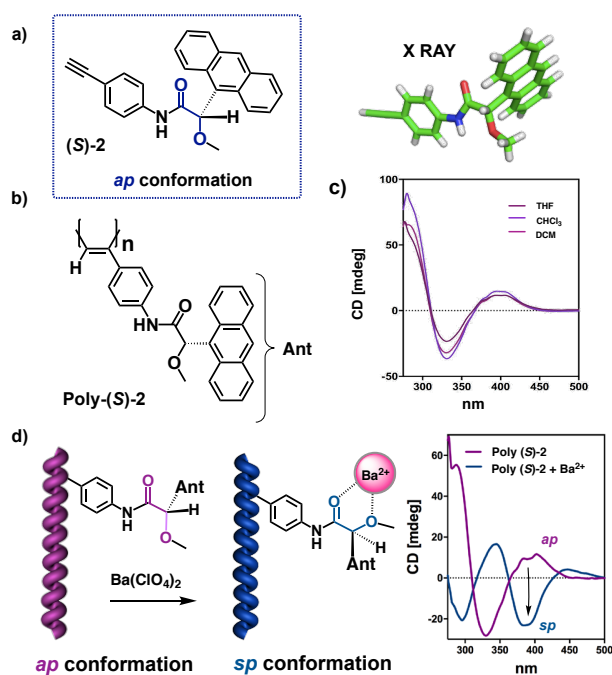


**Figure 4.** a) Chemical structure and X-ray of (S)-2. b) Chemical structure of poly-(S)-2. c) CD spectra of poly-(S)-2 in different solvents. d) Conformational *ap*/*sp* switch of poly-(S)-2 induced by Ba<sup>2+</sup> (external stimulus) and corresponding CD spectra in CHCl<sub>3</sub>.

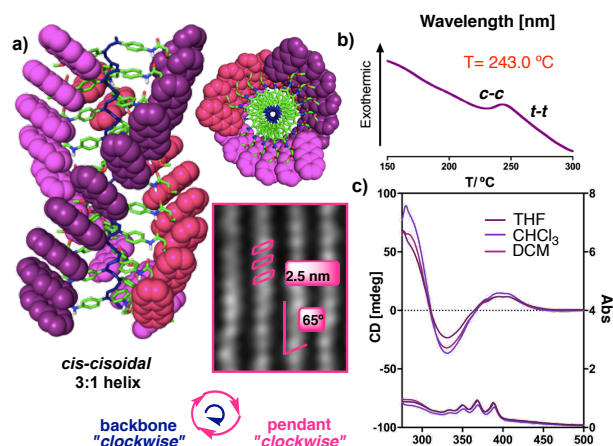


**Figure 5.** a) 3D structure and AFM image of poly-(S)-2 showing a *P*<sub>int</sub>/*P*<sub>ext</sub> helix. b) DSC thermogram of poly-(S)-2 showing a typical *cis-cisoidal* trace. c) CD studies of poly-(S)-2 showing a positive Cotton effect at the vinylic region.

Moreover, the presence of a positive Cotton effect at the vinylic region indicates also a *P* sense for the internal helix of the polymer in agreement with the presence of a *cis-cisoidal* polyene backbone<sup>12</sup> (Figure 5c). Hence, from these structural studies, we can conclude that poly-(S)-2 adopts a *cis-cisoidal* polyene backbone ( $\omega_1 = 65^\circ$ ) with the internal and the external helices rotating in the same direction [i.e., clockwise (*P*<sub>int</sub>/*P*<sub>ext</sub>)].

In summary, the homopolymers derived from monomers 1 and 2 present the same type of helical scaffold (*cis-cisoidal*,

$\omega=65^\circ$ ), although with different dynamic behavior: poly-**1** series are helical racemic due to a rapid equilibrium between the two helical senses, while poly-**2** presents clearly a prevalent helical sense, which can be tuned by the action of metal ions as external stimuli.

The similarity between the helical structures of poly-**1** and poly-**2** suggests<sup>2a</sup> that a copolymer formed by both mono-**1** and mono-**2** should constitute a good model to analyze the chiral communication through a fully chiral Sergeants and Soldiers effect, where the Sergeant can control the helical sense of the copolymer, independent of the (*R/S*)-Soldier chirality.

### Chiral-to-chiral communication studies

Different copolymers —poly[(*S*)-**1**<sub>r</sub>-co-(*S*)-**2**<sub>(1-r)</sub>], poly[(*R*)-**1**<sub>r</sub>-co-(*S*)-**2**<sub>(1-r)</sub>] and poly[(*rac*)-**1**<sub>r</sub>-co-(*S*)-**2**<sub>(1-r)</sub>],  $r=0.9-0.1$ — were prepared by polymerization of mixtures of the chiral Soldiers [(*S*)-**1**, (*R*)-**1**, (*rac*)-**1**] and the chiral Sergeant [(*S*)-**2**] with [(*Rh*(*nbd*)Cl)<sub>2</sub>] in different ratios (Figure 6).

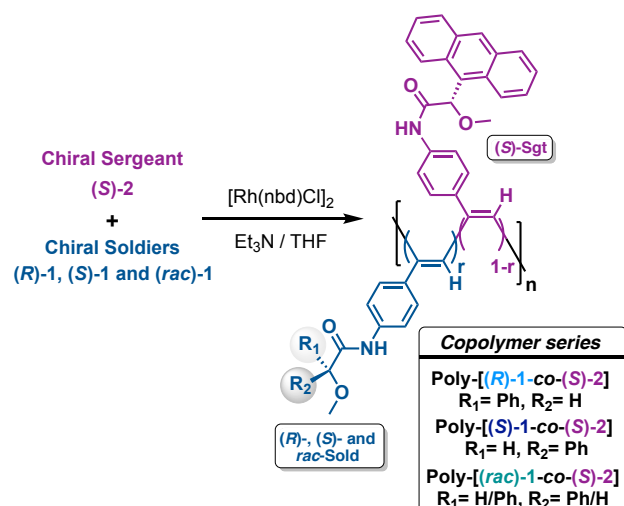


**Figure 6.** Monomer and copolymer structures used in this study.

All the copolymers showed by NMR (vinyl protons,  $\delta = 5.7-5.8$  ppm) and Raman (1567, 1335, 1003 cm<sup>-1</sup>) to possess a *cis* polyene backbone.<sup>9, 10</sup> Moreover, the DSC traces revealed as expected the presence of *cis-cisoidal* polyene backbones.<sup>13</sup> Their molecular weights were estimated by GPC (THF as eluent with polystyrene standards as calibrants; see SI for details) to be between Mn= 8000 and 12000 with Mn/Mw values around 1.5–2.5.

The chiral Soldier/chiral Sergeant monomer ratios in the copolymers were shown by NMR to be coincident with the feeding mixtures (see SI). Also, their random distribution within the chain was demonstrated by the Kelen-Tüdös method using varied monomer feed ratios and termination at low conversions<sup>14</sup> (see SI).

The CD spectra (0.3 mg/mL in THF) of poly-[(*S*)-**1**<sub>r</sub>-co-(*S*)-**2**<sub>(1-r)</sub>], poly-[(*R*)-**1**<sub>r</sub>-co-(*S*)-**2**<sub>(1-r)</sub>] and poly-[(*rac*)-**1**<sub>r</sub>-co-

(*S*)-**2**<sub>(1-r)</sub>] series showed, for all of them, CD curves analogous to that obtained from the poly-(*S*)-**2** homopolymer (Figure 7). In quantitative terms, the amount of Sergeant needed to induce a single-handed helix in the copolymer — maximum CD signal at the vinylic region — is close to 33%, meaning that each Sergeant unit is able to fix the conformation of two Soldiers.

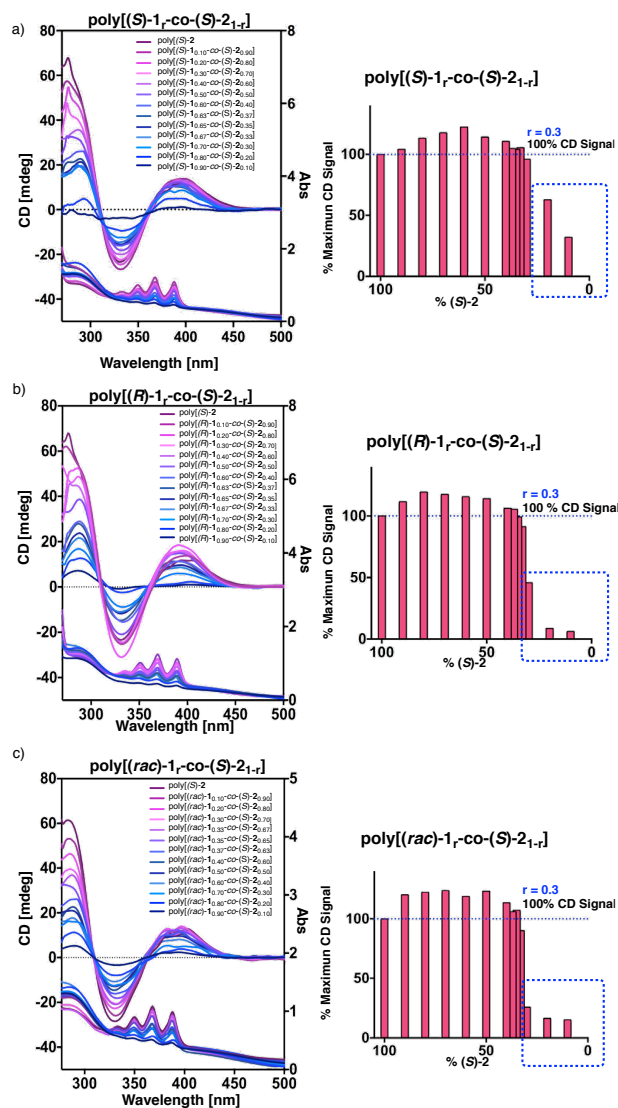


**Figure 7.** CD spectra and  $r$  values of the different copolymer series: (a) poly-[(*S*)-**1**<sub>r</sub>-co-(*S*)-**2**<sub>(1-r)</sub>], (b) poly-[(*R*)-**1**<sub>r</sub>-co-(*S*)-**2**<sub>(1-r)</sub>] and (c) poly-[(*rac*)-**1**<sub>r</sub>-co-(*S*)-**2**<sub>(1-r)</sub>].

Moreover, from these studies we may highlight that these copolymers respond to the classical Sergeant and Soldier effect but in a fully chiral system, where the chiral Sergeant [(*S*)-**2**] commands the chiral Soldier [(*S*)-**1**, (*R*)-**1**, (*rac*)-**1**] within the chain to adopt the right-handed *P* helix independently of the absolute configuration of the latter.

These results must follow different chiral to chiral communication mechanisms between the Sergeant and then two enantiomeric forms of the Soldier units. Thus, for instance, if the (*S*)-Sergeant [(*S*)-**2**] induces a certain preferred confor-



mation (conformation 1) into the (*S*)-Soldier [(*S*)-**1**], originating the *P* helical sense in the chain, a different conformation (conformation 2) has to be induced in the enantiomeric Soldier [(*R*)-**1**] to promote the same *P* helix. Moreover, when the Soldier is racemic [(*rac*)-**1**] the Sergeant should be able to command selectively two different conformations of the Soldier to promote a single handed helical structure into the copolymer —i.e., the Sergeant commands conformation 1 to the (*S*)-Soldier, while conformation 2 is induced in the (*R*)-Soldier—.

Important information related to these aspects was obtained from the interaction of the copolymers with metal ions. In poly-**1** homopolymers, containing MPA as pendant, it is well known that the 1:1 *sp/ap* conformational equilibrium of the chiral Soldier unit can be selectively shifted to either the *ap* or *sp* conformations by addition of monovalent and divalent metal ions respectively.<sup>7</sup> Those changes in the conformation of the pendants are transmitted to the helical backbone and can be monitored by CD studies through either inversion or amplification of the CD traces.

Hence, we test these experiments in the different copolymer series. When LiClO<sub>4</sub> was added to a THF solution of copolymer poly-[(*S*)-**1**<sub>0.60</sub>-*co*-(*S*)-**2**<sub>0.40</sub>], a slight chiral amplification was observed, while addition of Ba(ClO<sub>4</sub>)<sub>2</sub> produced a helical inversion (Figures 8a,b). This fact indicates that the chiral Soldier [(*S*)-**1**] in the native copolymer (Figure 9a) adopts an *ap* conformation, slightly improved by complexation with Li<sup>+</sup> but switched to the *sp* form by chelation with Ba<sup>2+</sup>.<sup>7</sup>

Analogous experiments on poly-[(*R*)-**1**<sub>0.60</sub>-*co*-(*S*)-**2**<sub>0.40</sub>] showed that LiClO<sub>4</sub> produced a helix inversion in the copolymer, while the addition of Ba(ClO<sub>4</sub>)<sub>2</sub> produced a slight helical enhancement (Figures 8c,d). Thus, in poly-[(*R*)-**1**<sub>*r*</sub>-*co*-(*S*)-**2**<sub>1-*r*</sub>], the chiral Soldier [(*R*)-**1**] adopts a preferred *sp* conformation (Figure 9b).<sup>7</sup>

Finally, in the poly-[(*rac*)-**1**<sub>*r*</sub>-*co*-(*S*)-**2**<sub>(1-*r*)</sub>] series, the (*R*)-**1** Soldiers have to adopt a *sp* conformation, while an *ap* conformation must be induced for the (*S*)-**1** ones to produce a helical enhancement in the copolymer (Figure 9c).

From a mechanistic point of view, we think that the effectiveness of the chiral Sergeant [(*S*)-**2**], inducing preferred and different conformations on each of the two possible absolute configurations of the chiral Soldier [(*R*)-**1** and (*S*)-**1**] is related to the ability of the anthryl group to generate  $\pi$ - $\pi$  stabilizing interactions with the Soldiers in either *ap* or *sp* forms (Figure 9).

Additionally, we decided to quantify this *chiral to chiral* Sergeant and Soldiers effect in the three different copolymer series studied —i.e., poly-[(*S*)-**1**<sub>*r*</sub>-*co*-(*S*)-**2**<sub>(1-*r*)</sub>], poly-[(*R*)-**1**<sub>*r*</sub>-*co*-(*S*)-**2**<sub>(1-*r*)</sub>] and poly-[(*rac*)-**1**<sub>*r*</sub>-*co*-(*S*)-**2**<sub>(1-*r*)</sub>]— using Sato's theory, which considers that the degree and direction of the helical sense induction depends on the nature of the neighboring monomer units.<sup>15,16</sup>

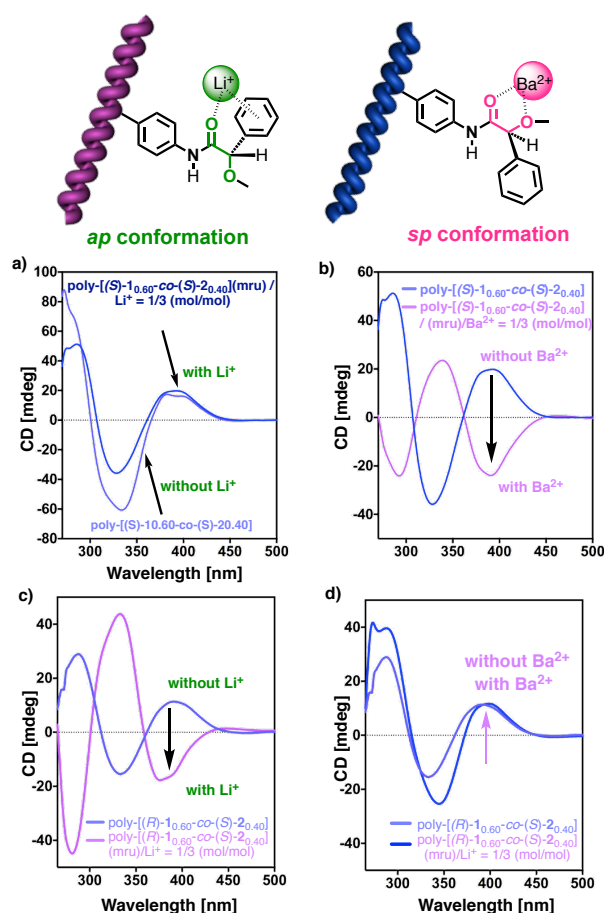


**Figure 8.** CD spectra of copolymer poly-[(*S*)-**1**<sub>0.6</sub>-*co*-(*S*)-**2**<sub>0.4</sub>] before and after the addition of (a) LiClO<sub>4</sub> and (b) Ba(ClO<sub>4</sub>)<sub>2</sub>. CD spectra of copolymer poly-[(*R*)-**1**<sub>0.6</sub>-*co*-(*S*)-**2**<sub>0.4</sub>] before and after the addition of (c) LiClO<sub>4</sub> and (d) Ba(ClO<sub>4</sub>)<sub>2</sub>.

Thus, two different energy preferences ( $\Delta G_h$ ) are considered related to the presence of a chiral Sergeant followed in sequence by another chiral Sergeant ( $\Delta G_{SS}$ ) or by a chiral Soldier ( $\Delta G_{Ss}$ )

$$g_{\text{abs}} = \tanh(-N\Delta G_h/RT)g_{\text{max}} \quad (1)$$

$$\Delta G_h = x^2\Delta G_{h,SS} + x(1-x)\Delta G_{h,Ss} \quad (2)$$

The  $g_{\text{abs}}$  obtained at 20°C was plotted against the mole fraction of the chiral Sergeant monomer and subjected to a nonlinear, least-squares fitting of the parameters  $\Delta G_{h,SS}$ ,  $\Delta G_{h,Ss}$ , and  $g_{\text{max}}$  using eqs 1 and 2 (Figure 10). The parameters could be converged successfully, affording  $\Delta G_{h,SS}$  and  $\Delta G_{h,Ss}$  values.

In the poly-[(*S*)-**1**<sub>*r*</sub>-*co*-(*S*)-**2**<sub>(1-*r*)</sub>] copolymer series, negative values of  $\Delta G_{h,SS} = -2.97$  and  $\Delta G_{h,Ss} = -0.24$  kJ/mol were obtained indicating that the same right-handed helical structure (*P* helix) is induced by the chiral Sergeant [(*S*)-**2**] and chiral Soldier [(*S*)-**1**] (Figure 10). In the case of the poly-[(*R*)-**1**<sub>*r*</sub>-*co*-(*S*)-**2**<sub>(1-*r*)</sub>] copolymer series, negative values of  $\Delta G_{h,SS} = -2.60$  and  $\Delta G_{h,Ss} = -0.17$  kJ/mol were obtained indicating again that the same right-handed helical structure (*P* helix) is in-

duced although is less energetically favored than in the poly-[(*S*)-1-*r*-co-(*S*)-2]<sub>1-*r*</sub>] copolymer series (Figure 10).

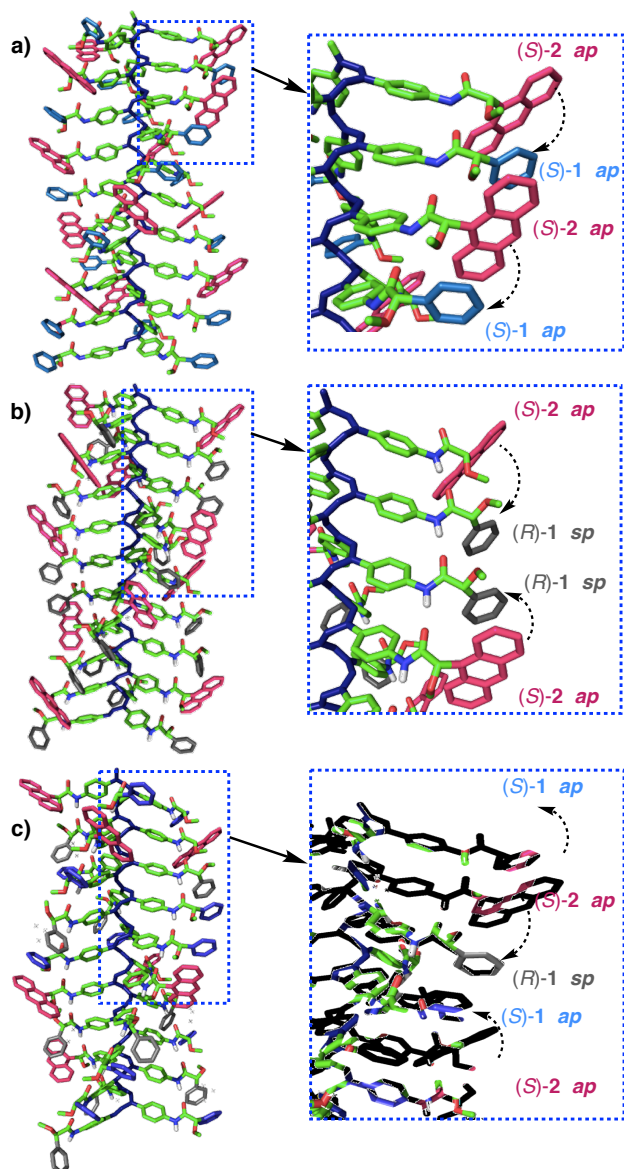


**Figure 9.** 3D model of the helical structures adopted by (a) poly-[(*S*)-1-*r*-co-(*S*)-2]<sub>1-*r*</sub>, (b) poly-[(*R*)-1-*r*-co-(*S*)-2]<sub>1-*r*</sub> and (c) poly-[(*rac*)-1-*r*-co-(*S*)-2]<sub>1-*r*</sub>, highlighting the conformational composition of the pendant groups.

Finally, the calculations on the poly-[(*rac*)-1-*r*-co-(*S*)-2]<sub>1-*r*</sub>, gave similar results to the previous case,  $\Delta G_{h,SS} = -2.58$  and  $\Delta G_{h,Ss} = -0.19$  kJ/mol, indicating that the *P* helical sense is also favored in these copolymer series but in a less effective way when compared to poly-[(*S*)-1-*r*-co-(*S*)-2]<sub>1-*r*</sub> (Figure 10).

These energy values are in good agreement with the *r*-values obtained for the Sergeants and Soldier effect in the copolymers —i.e., poly-[(*S*)-1-*r*-co-(*S*)-2]<sub>1-*r*</sub> *r* = 0.3, poly-[(*R*)-1-*r*-co-(*S*)-2]<sub>1-*r*</sub> *r* = 0.3 and poly-[(*rac*)-1-*r*-co-(*S*)-2]<sub>1-*r*</sub> *r* = 0.3— indicating that the Soldier with (*S*) configuration is the most "obedient" one.

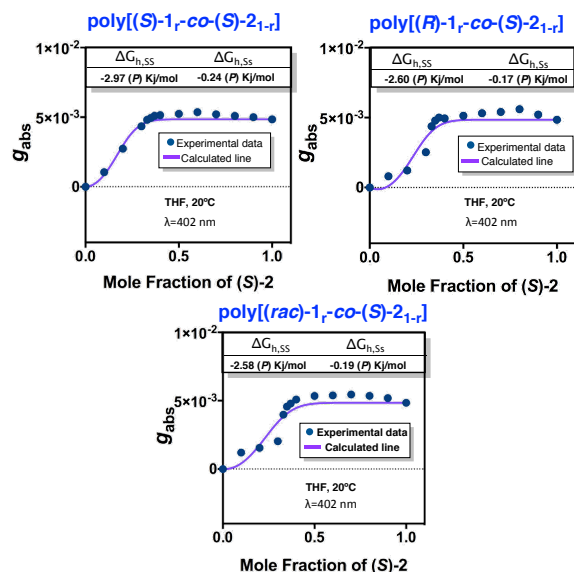


**Figure 10.** Plots of  $g_{abs}$  values at indicated wavelength of poly-[(*S*)-1-*r*-co-(*S*)-2]<sub>1-*r*</sub>, poly-[(*R*)-1-*r*-co-(*S*)-2]<sub>1-*r*</sub> and poly-[(*rac*)-1-*r*-co-(*S*)-2]<sub>1-*r*</sub> copolymer series against copolymer composition and their corresponding curve fitting based on eqs 1 and 2 to obtain the free energy parameters  $\Delta G_{h,SS}$  and  $\Delta G_{h,Ss}$ .

Finally, it is important to point out that all these copolymer series maintain intact their capacity to originate nanostructuration via helical polymer-metal complexes (HPMCs).<sup>7d</sup> For instance, poly-[(*rac*)-1<sub>0.67</sub>-co-(*S*)-2]<sub>0.33</sub> (conc = 0.3 mg/mL in CHCl<sub>3</sub>) originated stable and well-defined spherical particles when treated with Ba<sup>2+</sup> and Ag<sup>+</sup>. Both the divalent and monovalent cations were added as perchlorates in MeOH (*mru*/*M*<sup>n+</sup> = 1.0/0.2 mol/mol) and the resulting tunable nanospheres showed very good sizes and PDI values (61 nm, 0.071 and 74 nm and 0.067 respectively) (Figure S17) and preserved the encapsulating properties of these systems.<sup>7d</sup>

## CONCLUSIONS

In conclusion, we have describe six helical copolymer series constituted by two chiral components that respond to the classical Sergeants and Soldiers effect and where ten different helices can be prepared from four different stereochemical combinations: *P*/*M* helical sense of the backbone and *R*/*S* chirality of the groups at the periphery (Figure 11). The helical sense is exclusively determined by the absolute configuration of the Sergeant (minor component) while the chirality at the periphery is determined by the absolute configuration of the Soldier (major component). In addition, the helical sense of four of these six helical copolymers can be selectively inverted or enhanced by the addition of metal ions as external stimuli (Figure 11). In this way, helical polymers with clockwise (or counterclockwise) helical sense and (*R*)- or (*S*)-chirality at the external part can be produced and the helix inverted to the opposite counterclockwise (or clockwise) sense while maintaining the chiral decoration at the surface. From a structural point of view, this helical induction

is due to the unique interactions between the large anthryl groups of the Sergeants and the vicinal Soldier units that shift their conformation to favor  $\pi$ - $\pi$  stacking that stabilize the helix. Additionally, these chiral copolymers form HPMCs that originate nanospheres with encapsulating properties when treated with appropriate metal salts.

According with our results, the design of a copolymer with this behavior requires: i) Sergeant and Soldier producing homopolymers with resembled scaffolds, i.e., similar dihedral angles for conjugated double bonds; ii) a Sergeant with a preferred single conformation and a highly extended aromatic ring, and finally iii) a Soldier with a highly dynamic conformational equilibrium between two conformations.

This novel approach to helical structures with controlled helicity ( $P$  or  $M$ ) even after changes on the chirality of the major component of the copolymer [( $R$ )-, ( $S$ )- or rac-Sold.], will open new avenues towards the rational design and production of new chiroptical materials, where the role of the helix and the role of the chirality at the pendant groups could be explored independently.

## ASSOCIATED CONTENT

### Supporting Information.

Materials and methods, synthesis and characterization of monomers, synthesis and characterization copolymers, conformational studies, AFM studies, nanostructuration studies and supporting references.

The Supporting Information is available free of charge on the ACS Publications website.

## AUTHOR INFORMATION

### Corresponding Author

ricardo.riguera@usc.es, felix.freire@usc.es

### Funding Sources

No competing financial interests have been declared.

## ACKNOWLEDGMENT

Financial support from MINECO (CTQ2014-61470-EXP, CTQ2015-70519-P), Xunta de Galicia (GRC2014/040, Centro singular de investigación de Galicia accreditation 2016-2019, ED431G/09) and the European Regional Development Fund (ERDF) is gratefully acknowledged. We also thank Servicio de Nanotecnología y Análisis de Superficies (CACTI, UVIGO).

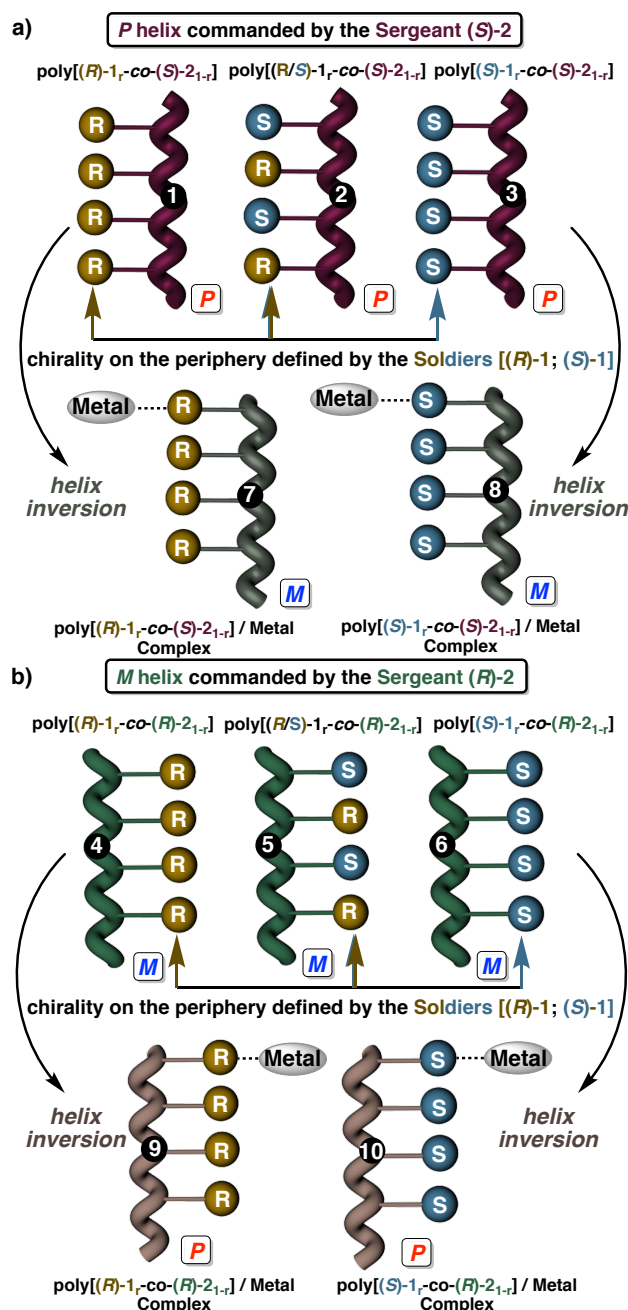


**Figure 11.** (a) Graphical illustration of the helical structures of poly-[( $R$ )- $1_r$ -co-( $S$ )- $2_{(1-r)}$ ] (1), poly-[( $rac$ )- $1_r$ -co-( $S$ )- $2_{(1-r)}$ ] (2) and poly-[( $S$ )- $1_r$ -co-( $S$ )- $2_{(1-r)}$ ] (3) showing identical scaffold and helical sense ( $P$  helix) but different composition at the periphery. The  $M$  helices obtained by helical inversion are also shown (7 and 8). (b) Idem for poly-[( $R$ )- $1_r$ -co-( $R$ )- $2_{(1-r)}$ ] (4), poly-[( $rac$ )- $1_r$ -co-( $R$ )- $2_{(1-r)}$ ] (5) and poly-[( $S$ )- $1_r$ -co-( $R$ )- $2_{(1-r)}$ ] (6) showing identical scaffold and helical sense ( $M$  helix) but different composition at the periphery. The  $P$  helices obtained by helical inversion are also shown (9 and 10).

## REFERENCES

- (1) (a) Xu, A.; Masuda, T.; Zhang, A. *Polym. Rev.* 2017, 57, 138. (b) Yashima, E.; Ousaka, N.; Taura, D.; Shimomura, K.; Ikai, T.; Maeda, K. *Chem. Rev.* 2016, 116, 13752. (c) Freire, F.; Quiñoá, E.; Riguera, R. *Chem.*



- Rev. 2016, 116, 1242. (d) Yashima, E.; Maeda, K.; Lida, H.; Furusho, Y.; Nagai, K. *Chem. Rev.* 2009, 109, 6102. (e) Liu, J.; Lam, J. W. Y.; Tang, B. Z. *Chem. Rev.* 2009, 109, 5799. (f) Yashima, E.; Maeda, K.; Furusho, Y. *Acc. Chem. Res.* 2008, 41, 1166. (g) Rudick, J. G.; Percec, V. *Acc. Chem. Res.* 2008, 41, 1641. (h) Yashima, E.; Maeda, K. *Macromolecules* 2008, 41, 3. (i) Yashima, E.; Maeda, K. *Helically Folding Polymers in Foldamers: Structure Properties and Applications*; Eds: Hecht, S.; Huc, I. WILEY-VCH, Weinheim, 2007, pp 331. (j) Maeda, K.; Yashima, E. *Top. Curr. Chem.* 2006, 265, 47.
- (2) (a) Arias, S.; Rodríguez, R.; Quiñoá, E.; Riguera, R.; Freire, F. J. *Am. Chem. Soc.* 2018, 140, 667. (b) Arias, S.; Bergueiro, J.; Freire, Quiñoá, E.; Riguera, R. *Small*, 2016, 12, 238. (c) Nagata, Y.; Nishikawa, T.; Sugimoto, M. *ACS Macro Lett.*, 2016, 5, 519. (d) Nagata, Y.; Nishikawa, T.; Sugimoto, J. *Am. Chem. Soc.*, 2015, 137, 4070. (e) Bergueiro, J.; Freire, F.; Wandler, E. P.; Seco, J. M.; Quiñoá, E.; Riguera, R. *Chem. Sci.* 2014, 5, 2170. (f) Jain, V.; Cheon, K.-S.; Tang, K.; Jha, S.; Green, M. M. *Isr. J. Chem.* 2011, 51, 1067. (g) Jain, V.; Cheo, K. -S.; Tang, Jha, S.; Green M. M. *Angew. Chem., Int. Ed.* 2011, 51, 1067. (h) Mateos-Timoneda, M. A.; Crego-Calama, M.; Reinhoud, D. N. *Chem. Soc. Rev.*, 2004, 33, 363. (i) Tang, K.; Green, M. M.; Cheon, K. S.; Selinger, J. V.; Garetz, B. A. *J. Am. Chem. Soc.*, 2003, 125, 7313. (j) Green, M. M.; Park, J. W.; Sato, T.; Teramoto, A.; Lifson, S.; Selinger, R. L.; Selinger, J. V. *Angew. Chem., Int. Ed.* 1999, 38, 3139. (k) Gu, H.; Nakamura, Y.; Sato, T.; Teramoto, A.; Green, M. M.; Jha, S. K.; Andreola, C.; Reidy, M. P. *Macromolecules* 1998, 31, 6362. (l) Green, M. M.; Peterson, N. C.; Sato, T.; Teramoto, A.; Cook, R.; Lifson, S. *Science* 1995, 268, 1860. (m) Green, M. M.; Reidy, M. P.; Johnson, R. D.; Darling, G.; O'Leary, D. J.; Willson, G. J. *Am. Chem. Soc.* 1989, 111, 6452.
- (3) (a) Maeda, K.; Hirose, D.; Okoshi, N.; Shimomura, K.; Wada, Y.; Ikai, T.; Kanoh, S.; Yashima, E. *J. Am. Chem. Soc.* 2018, 140, 3270. (b) Shimomura, K.; Ikai, T.; Kanoh, S.; Yashima, E.; Maeda, K. *Nat. Chem.* 2014, 6, 429.
- (4) (a) Ke, Y.-Z.; Nagata, Y.; Yamada, T.; Sugimoto, M. *Angew. Chem. Int. Ed.* 2015, 54, 9333. (a) Yamamoto, T.; Yamada, T.; Nagata, Y.; Sugimoto, M. *J. Am. Chem. Soc.* 2010, 132, 789.
- (5) (a) Zhao, B.; Chen, C.; Huang, H.; Deng, J. *Colloid. Polym. Sci.* 2015, 293, 349. (b) Zhang, H.; Song, J.; Deng, J. *Macromol. Rapid Commun.* 2014, 35, 1216.
- (6) (a) Takei, F.; Onitsuka, K.; Takahashi, S.; Terao, K.; Sato, T. *Macromolecules* 2007, 40, 5245. (b) Tabei, J.; Shiotsuki, M.; Sato, T.; Sanda, F.; Masuda, T. *Chem. Eur. J.* 2005, 11, 3591. (c) Deng, J. P.; Tabei, J.; Shiotsuki, M.; Sanda, F.; Masuda, T. *Macromolecules* 2004, 37, 9715. (d) Morino, K.; Maeda, K.; Okamoto, Y.; Yashima, E.; Sato, T. *Chem. Eur. J.* 2002, 8, 5112. (e) Koe, J. R.; Fujiki, M.; Motonaga, M.; Nakashima, H. *Macromolecules* 2001, 34, 1082. (f) Maeda, K.; Okamoto, Y. *Macromolecules* 1999, 32, 974.
- (7) (a) Rodríguez, R.; Arias, S.; Quiñoá, E.; Riguera, R.; Freire, F. *Nanoscale*, 2017, 9, 17752. (b) Arias, S.; Freire, F.; Quiñoá, E.; Riguera, R. *Polym. Chem.* 2015, 6, 4725. (c) Arias, S.; Freire, F.; Quiñoá, E.; Riguera, R. *Angew. Chem., Int. Ed.* 2014, 53, 13720. (d) Freire, F.; Seco, J. M.; Quiñoá, E.; Riguera, R. *J. Am. Chem. Soc.* 2012, 134, 19374. (e) Freire, F.; Seco, J. M.; Quiñoá, E.; Riguera, R. *Angew. Chem., Int. Ed.* 2011, 50, 11692.
- (8) (a) Freire, F.; Seco, J. M.; Quiñoá, E.; Riguera, R. *Org. Lett.*, 2010, 12, 208. (b) Freire, F.; Quiñoá, E.; Riguera, R. *Chem. Commun.* 2007, 14, 1456.
- (9) (a) Li, B. S.; Lam, J. W. Y.; Yu, Z.-Q.; Tang, B. Z. *Langmuir* 2012, 28, 5770. (b) Louzao, I.; Seco, J. M.; Quiñoá, E.; Riguera, R. *Angew. Chem. Int. Ed.* 2010, 49, 1430. (c) Sakurai, S. I.; Okoshi, K.; Kumaki, J.; Yashima, E. *Angew. Chem., Int. Ed.* 2006, 45, 1245. (d) Li, B. S.; Kang, S. Z.; Cheuk, K. K. L.; Wan, L.; Ling, L.; Bai, C.; Tang, B. Z. *Langmuir* 2004, 20, 7598.
- (10) (a) Cheuk, K. K. L.; Li, B. S.; Lam, J. W. Y.; Xie, Y.; Tang, B. Z. *Macromolecules* 2008, 41, 5997. (b) Mayershofer, M. G.; Nuyken, O. *J. Polym. Sci., Part A: Polym. Chem.* 2005, 43, 5723. (c) Li, B. S.; Cheuk, K. K. L.; Ling, L.; Chen, J. X. X.; Baiand, C.; Tang, B. Z. *Macromolecules* 2003, 36, 77. (d) Cheuk, K. K. L.; Lam, J. W. Y.; Lai, L. M.; Dongand, Y.; Tang, B. Z. *Macromolecules* 2003, 36, 9752.
- (11) (a) F. Freire, E. Quiñoá, R. Riguera, *Chem. Commun.*, 2017, 53, 481. (b) R. Rodríguez, J. Ignés-Mullol, F. Sagués, E. Quiñoá, R. Riguera, F. Freire, *Nanoscale*, 2016, 8, 3362. (c) S. I. Sakurai, S. Ohsawa, K. Nagai, K. Okoshi, J. Kumaki, E. Yashima, E. *Angew. Chem., Int. Ed.*, 2007, 46, 7605.
- (12) Fernández, B.; Rodríguez, R.; Rizzo, A.; Quiñoá, E.; Riguera, R.; Freire, F. *Angew. Chem. Int. Ed.* 2018, 57, 3666.
- (13) Liu, L.; Namikoshi, T.; Zang, Y.; Aoki, T.; Hadano, S.; Abe, Y.; Wasuzu, I.; Tsutsuba, T.; Teraguchi, M.; Kaneko, T. *J. Am. Chem. Soc.* 2013, 135, 602.
- (14) (a) K. Maeda, M. Muto, T. Sato, E. Yashima, *Macromolecules*, 2011, 44, 8343. (b) T. Kelen, F. Tüd.s, J. *Macromol. Sci. Chem.*, 1975, 9, 1.
- (15) Lifson S.; Andreola, C.; Peterson, N. C.; Green, M. M. *J. Am. Chem. Soc.* 1989, 111, 8850.
- (16) (a) F. Takei, K. Onitsuka, S. Takahashi, K. Terao, T. Sato, *Macromolecules* 2007, 40, 5245. (b) J. Tabei, M. Shiotsuki, T. Sato, F. Sanda, T. Masuda, *Chem. Eur. J.* 2005, 11, 3591.

TOC

